The Design of Coupled Microstrip Lines

SINA AKHTARZAD, THOMAS R. ROWBOTHAM, AND PETER B. JOHNS

Abstract—**Although graphical results and formulas are available for the design of microstrip couplers, the design procedure is hampered because even- and odd-mode impedances are always expressed in terms of the physical geometry. In practice the designer obtains these impedances and then requires to know the geometry given by them.**

A new design procedure for coupled parallel microstrip lines is therefore presented. The technique enables the geometry of the coupled lines to be obtained directly from the required even- and odd-mode impedances and uses single microstrip-line geometry as an intermediate step. The results are presented in graphical form using only two universal families of curves. Results are also presented in the form of simple formulas for design programs and also comparisons with practical results are made.

I. NOMENCLATURE

Z_{0e}, Z_{0o}	Even- and odd-mode characteristic impedance of the coupled microstrip lines.
Z_0	Characteristic impedance of the equivalent single microstrip line.
$W/H, S/H$	Shape ratio (width-to-substrate thickness and gap between lines to substrate thickness) for the coupled microstrip lines.
$(W/H)_s, (W/H)_{se}, (W/H)_{so}$	Shape ratio for the equivalent single line—general case, corresponding to even-mode geometry, corresponding to odd-mode geometry.
ϵ_r	Substrate relative permittivity.

II. INTRODUCTION

THE DESIGN of parallel-line microstrip couplers and filters requires a relationship between the geometry of the device (see Fig. 1) and the even- and odd-mode characteristic impedances (Z_{0e} and Z_{0o}). Curves are available [1], [2] for Z_{0e} and Z_{0o} plotted against W/H amd S/H and design procedure requires a search for those particular W/H and S/H values which simultaneously yield Z_{0e} and Z_{0o}. Interpolation between different sets of curves for different substrate permittivities is also required. These curves may be generated using formulas which are now available [3], but these tend to be quite lengthy and do not lend themselves to easy simultaneous solution.

This paper describes a procedure whereby the designer can calculate W/H and S/H from desired values of Z_{0e} and Z_{0o} either using just two universal graphs or with the aid of a computer. In both cases there are two steps. One of these uses the well-known relationship for the characteristic impedance of a single line in terms of its shape ratio $(W/H)_s$. The other step to be described relates W/H and S/H (for the coupled lines) to $(W/H)_s$ (the intermediate single-line geometry). The latter results may be made independent of the permittivity and are given not only in graphical form but also as simple formulas.

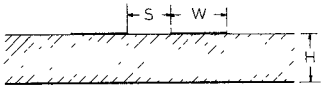

Fig. 1. The geometry of coupled microstrip lines.

III. DESIGN PROCEDURES

A. Synthesis

In the synthesis procedure, Z_{0e} and Z_{0o} for the coupled lines are known and it is required to find W/H and S/H. The first step is to find the two single-line shape ratios $(W/H)_{se}$ and $(W/H)_{so}$ corresponding to the impedance $Z_{0e}/2$ and $Z_{0o}/2$, respectively. Wheeler's theory [4] provides curves, reproduced in Fig. 2, for obtaining these shape ratios graphically or alternatively, Wheeler's synthesis formula may be used

$$(W/H)_s = (2/\pi)(d-1) - (2/\pi)\log_e(2d-1) + \frac{(\epsilon_r - 1)}{\pi\epsilon_r}\left(\log_e(d-1) + 0.293 - \frac{0.517}{\epsilon_r}\right) \quad (1)$$

where

$$d = \frac{60\pi^2}{Z_0(\epsilon_r)^{1/2}}.$$

The values of $(W/H)_s$ used in this technique are always large enough for the curves of Fig. 2 or (1) to apply with good accuracy.

W/H and S/H for the coupled lines are now found by simultaneous solution of the following formulas:

$$(W/H)_{se} = (2/\pi)\cosh^{-1}\left(\frac{2h - g + 1}{g + 1}\right) \quad (2)$$

$$(W/H)_{so} = (2/\pi)\cosh^{-1}\left(\frac{2h - g - 1}{g - 1}\right) + \frac{4}{\pi(1 + \epsilon_r/2)}\cosh^{-1}\left(1 + 2\frac{W/H}{S/H}\right), \quad \epsilon_r \leq 6 \quad (3)$$

Manuscript received March 15, 1974; revised December 3, 1974.

S. Akhtarzad and P. B. Johns are with the Department of Electrical and Electronic Engineering, University of Nottingham, Nottingham, England.

T. R. Rowbotham is with the Post Office Research Department, Martlesham, Heath, Suffolk, England.

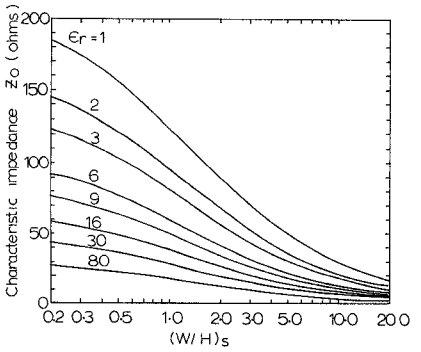

Fig. 2. Single microstrip line characteristic impedance [4].

$$(W/H)_{so} = (2/\pi)\cosh^{-1}\left(\frac{2h - g - 1}{g - 1}\right) + (1/\pi)\cosh^{-1}\left(1 + 2\frac{W/H}{S/H}\right), \qquad \epsilon_r \geq 6$$

where

$$g = \cosh\left[\tfrac{1}{2}\pi(S/H)\right]$$

and

$$h = \cosh\left[\pi(W/H) + \tfrac{1}{2}\pi(S/H)\right].$$

Equations (2) and (3) are given in graphical form in Fig. 3 where the curves are plotted for a fixed value of permittivity $\epsilon_r = 6$. The relationship to a single microstrip line cannot be made independent of the permittivity, but the formula with $\epsilon_r = 6$ gives accurate results for substrates with permittivity $\epsilon_r = 6$ and above. For permittivities down to $\epsilon_r = 2$, the formula for $\epsilon_r = 6$ (plotted in Fig. 3) has errors up to about 10 percent for the worst S/H and W/H values. For greater accuracy at low permittivities and certainly for values of permittivity less than $\epsilon_r = 2$ the equation for $\epsilon_r \leq 6$ should be used, and in this case it will be noticed that ϵ_r appears as a variable.

The solution of simultaneous equations (2) and (3) is greatly eased by ignoring the second term in (3). A value of S/H is then given directly by

$$S/H = (2/\pi)\cosh^{-1}\cdot\left\{\frac{\cosh\left[\tfrac{1}{2}\pi(W/H)_{se}\right] + \cosh\left[\tfrac{1}{2}\pi(W/H)_{so}\right] - 2}{\cosh\left[\tfrac{1}{2}\pi(W/H)_{so}\right] - \cosh\left[\tfrac{1}{2}\pi(W/H_{se}\right]}\right\}. \quad (4)$$

Substitution into (2) and (3) of the values obtained from (4) will show that in most cases (4) is sufficiently accurate. If this substitution is not sufficiently accurate (and this may happen, particularly at lower values of permittivity) then (4) provides a useful starting point for an optimization process in the solution of (2) and (3).

B. Analysis

In the analysis procedure, W/H and S/H for the coupled lines are known and it is required to find Z_{0e} and Z_{0o}. Here the first step is to find the two single-line shape ratios $(S/H)_{se}$ and $(W/H)_{so}$ corresponding to W/H and S/H for the even and odd modes, respectively. These are obtained from (2) and (3) or from Fig. 4 which is again plotted for $\epsilon_r = 6$ (see Section III-A). The characteristic impedances (Z_0) for a single strip corresponding to the shape ratios $(W/H)_{se}$ and $(W/H)_{so}$ are now required. These may be obtained from Fig. 2 or alternatively, the corresponding analysis formula may be used

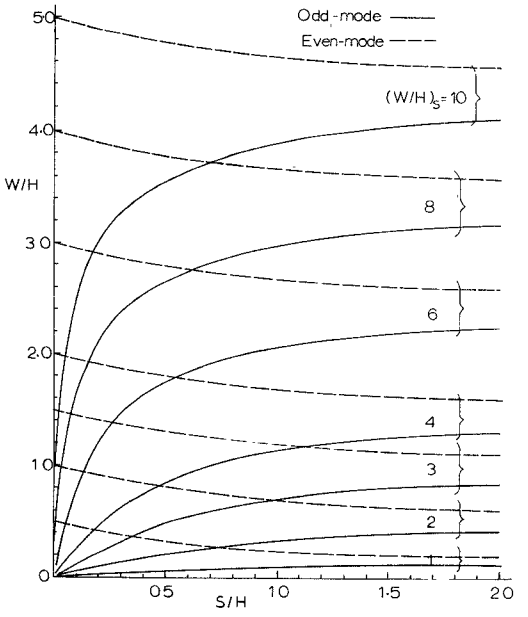

Fig. 3. Synthesis curves for coupled microstrip lines.

$$Z_0 = \frac{120\pi(1/\epsilon_r)^{1/2}}{(W/H)_s + 0.882 + [(\epsilon_r + 1)/\pi\epsilon_r]\{\log_e(W/H)_s + 1.88) + 0.758\} + [(\epsilon_r - 1)/\epsilon_r^2](0.164)}.$$

Alternative formulas for this result are given in [5].

The even- and odd-mode impedances are then given by

$$Z_{0e} = 2Z_0 \quad \text{(for shape ratio } (W/H)_{se})$$

$$Z_{0o} = 2Z_o \quad \text{(for shape ratio } (W/H)_{so}).$$

C. Wave Velocity

The phase velocity for waves on a structure with even-mode excitation will be different from the velocity on a structure with odd-mode excitation. In practical design procedure it is usual to take the mean value of these two velocities.

The even-mode velocity (v) may be obtained from the single-line equivalent characteristic impedance for even mode (Z_0) using the following formula:

$$\frac{v}{c} = \frac{Z_0}{(Z_0)_{\epsilon_r=1}}$$

where c and $(Z_0)_{\epsilon_r=1}$ are the phase velocity and characteristic impedance in the same equivalent structure, but with substrate permittivity equal to free space $(\epsilon_r = 1)$. A similar calculation gives the odd-mode velocity.

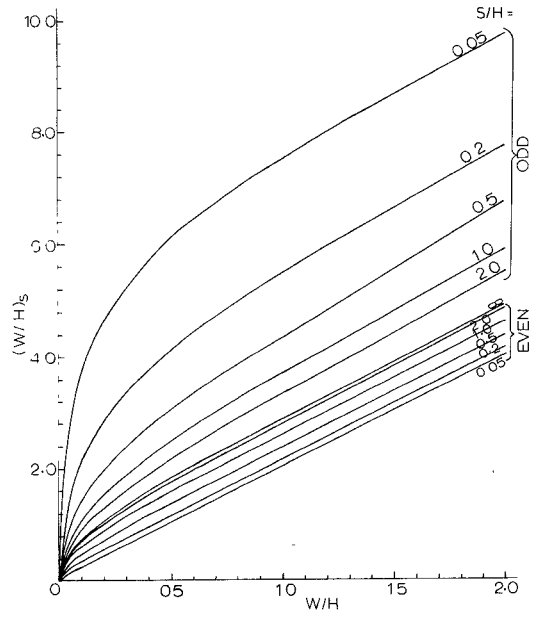

Fig. 4. Design curves for coupled microstrip lines.

IV. DERIVATION OF RESULTS

A. Conformal Mapping

Equations (2) and (3) or Fig. 4 give the width of a single microstrip line which would have the same characteristic impedance between line and gound as the two separate lines in the coupled-line configuration. The single microstrip line is used as an intermediate step in the calculation because the field fringing effects at the edges of the single microstrip line are very similar to the fringing effects on the outside edges of the coupled lines. By taking the single-line equivalent, therefore, the inductance and capacitance effects (both in air and dielectric) of the outside edges of the coupled lines are properly accounted for.

The additional complication in the coupled-line geometry is the field fringing in the region of the gap between the lines (the inside edges). It is assumed initially that this fringing field in the gap lies totally in the dielectric. This assumption is attractive for the following two reasons.

1) The calculation of the geometry of the single-line equivalent of the coupled lines may be made independent of the permittivity of the dielectric. In other words, the only inhomogeneous part of the problem lies at the outside edges of the coupled lines and this is properly accounted for when using the published solution for the single-line geometry (these are not independent of permittivity, of course).

2) The calculation procedure can be performed using a simple conformal mapping procedure which maps only the dielectric region of the coupled-line geometry in the z plane to the w plane. Adjustments are made only to those regions in the w plane which involve the gap and then the geometry is transformed back to the z plane. Thus there is no harm in placing an open-circuit boundary along the face of the dielectric for transformation purposes provided the problem finally returns to the original z plane where the boundary condition can be removed again. Since the calculations concerning the gap are performed under homogeneous conditions, it is necessary only to discuss the capacitance effects; the inductance effects will automatically be correct.

In the even-mode case it will be shown that the assumption that the fields lie totally in the dielectric is quite reasonable. In the odd-mode case, however, errors arise from this assumption and the formulas are then adjusted taking due regard of the inhomogeneous nature of the problem.

It is required to map the degenerate triangle in the z plane shown in Fig. 5(a) into the upper half of the w plane shown in Fig. 5(b). This is accomplished by the Schwarz–Christoffel transformation which for the general case of a polygon may be expressed as [6]

$$z = z_0 + A \int (w - b_0)^{-\phi_0/\pi}(w - b_1)^{-\phi_1/\pi} \cdots dw. \qquad (5)$$

The angle at $z = j\infty$ is zero and the remaining two angles at $z = -\pi/2$ and $z = +\pi/2$ are each $\pi/2$. Placing b_1 at $w = -1$ and b_2 at $w = +1$, (5) becomes

$$z = z_0 + A \int \frac{dw}{(w^2 - 1)^{1/2}}$$

$$= z_0 + A \cosh^{-1} w.$$

Now when

$$z = \pi/2 \quad \text{then} \quad w = +1 \quad \text{and} \quad z_0 = \pi/2.$$

Also when

$$z = -\pi/2 \quad \text{then} \quad w = -1 \quad \text{and} \quad A = -j.$$

Thus the required transformation is

$$w = \sin z. \qquad (6)$$

B. Even-Mode Geometry

Fig. 6(a) shows the coupled-line even-mode geometry. The potential is constant along the full lines, and the normal gradient of the potential is taken as zero along the broken lines. This neglects any fringing field in the air at A, an approximation which will be discussed later. The transformation (6) into the w plane is shown in Fig. 6(b). The exercise of scaling into the w' plane now requires the positive half of the w' plane to remain unchanged while the gap AF is reduced to zero.

If

$$-g = \sin\left[-\tfrac{1}{2}\pi + j(\tfrac{1}{2}\pi)(S/H)\right]$$

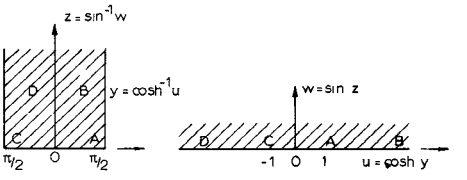

Fig. 5. Schwarz–Christoffel transformation. (a) z plane. (b) w plane.

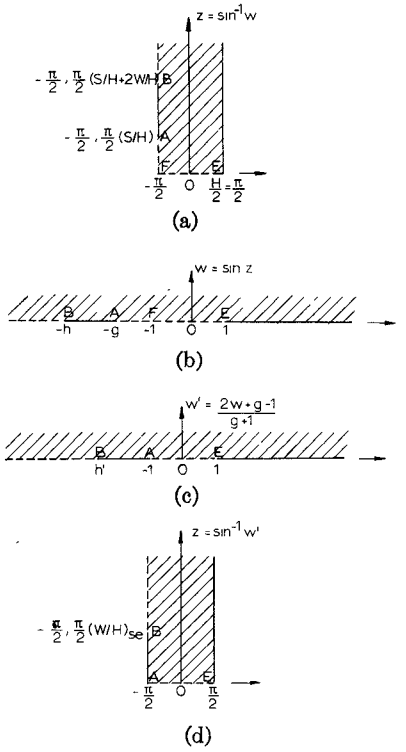

Fig. 6. Transformations for even-mode geometry. (a) z plane. (b) w plane. (c) w' plane. (d) z plane.

i.e.,

$$g = \cosh\left[\tfrac{1}{2}\pi(S/H)\right]$$

then the required scaling transform, shown in Fig. 6(c), is

$$w' = \frac{2w + g - 1}{g + 1}$$

since, for $w = 1$, $w' = 1$, and for $w = -g$, $w' = -1$.

Fig. 6(d) shows the transformation back to the z plane. For

$$h = \cosh\left[\pi(W/H) + \tfrac{1}{2}\pi(S/H)\right]$$

the required width of the strip $(W/H)_{se}$ is given by

$$-\left(\frac{2h - g + 1}{g + 1}\right) = \sin\left[-\tfrac{1}{2}\pi + j(\tfrac{1}{2}\pi)(W/H)_{se}\right] \quad (7)$$

which gives (2).

The physical interpretation of this result can be seen with the aid of Fig. 6(a). The total capacitance is made up of the parallel-plate capacitance AB to ground, the fringing capacitance at B (which is constant over a large range of W/H and S/H), and the fringing capacitance at A (which varies considerably with S/H). A single line has fringing capacitance only at B. Therefore, a single line which has the same capacitance as the pair of coupled lines must be wider than $2(W/H)$ by an amount which takes account of the fringing capacitance at A. This factor varies considerably with S/H when S/H is small but settles to a constant value when S/H becomes large enough for the fringing field to be unaffected by the adjacent line. Thus the even-mode section of Fig. 4 shows that (2) approximates to parallel straight lines of slope 2 for most of the W/H range.

For $S/H = 0$, (2) becomes

$$(W/H)_{se} = 2(W/H)$$

which is expected since the fringing field at A has reduced to zero.

For $S/H \to \infty$ and writing

$$(W/H)_{se} = m(W/H) + k$$

(2) approximates to

$$\cosh\left[m(\tfrac{1}{2}\pi)(W/H) + k(\tfrac{1}{2}\pi)\right] = 2[\cosh \pi(W/H) + \sinh \pi(W/H)] - 1.$$

For large W/H this gives

$$k = \frac{2 \log_e 4}{\pi} = 0.88.$$

This is the constant increase in W/H which accounts for the fringing field at A for very large S/H. It is under these conditions of large S/H that maximum error will occur due to neglecting the fringing field in the air at A. [Note that the fringing field at B is always properly accounted for when using (1)]. A comparison with the results of [1] and [2] and direct comparison with the edge-effect results of [7] shows that neglecting the fringing field in the air produces negligible error.

C. Odd-Mode Geometry

In the first instance the procedure for the odd mode is similar to that used in the even mode. Referring to Fig. 7, it can be seen that the scaling transform this time is given

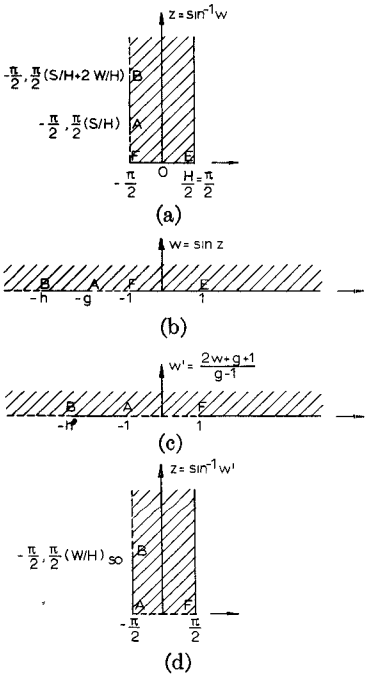

Fig. 7. Transformations for odd-mode geometry. (a) z plane. (b) w plane. (c) w' plane. (d) z plane.

by

$$w' = \frac{2w + g + 1}{g - 1}$$

since this time for $w = -1$, $w' = 1$, and for $w = -g$, $w' = -1$.

Transferring back to the z plane, the width $(W/H)_{so}$ is given by

$$-\left(\frac{2h - g - 1}{g - 1}\right) = \sin\left[-\tfrac{1}{2}\pi + j(\tfrac{1}{2}\pi)(W/H)_{so}\right] \quad (8)$$

which gives the first term of (3).

Again, that part of the fringing field at A which is in the air has been neglected and, whereas this did not affect the accuracy in the even-mode case, larger errors can occur in the odd-mode case. The inaccuracies are most pronounced when S/H is small and where the substrate relative permittivity is near unity. In order to account for this extra fringing field, the width of an equivalent single line must be increased over and above that given by (8). It is required therefore to find the width of the parallel-plate capacitor, distance H between the plates, which has the same capacitance as that caused by the fringing field in the air at A. This capacitor, when inserted into the middle of the single equivalent strip, will increase the width by the correct amount.

The geometry of the problem is shown in Fig. 8, this time in the w plane where the capacitance of one of the lines to ground is twice the capacitance between the pair of lines shown. The scaling transform to the w' plane is now given by

$$w' = w \times (2/S).$$

This gives in the z plane

$$[1 + 2(W/S)] = \sin\left[\tfrac{1}{2}\pi + j(\tfrac{1}{2}\pi)(W/H)_{so}\right]$$

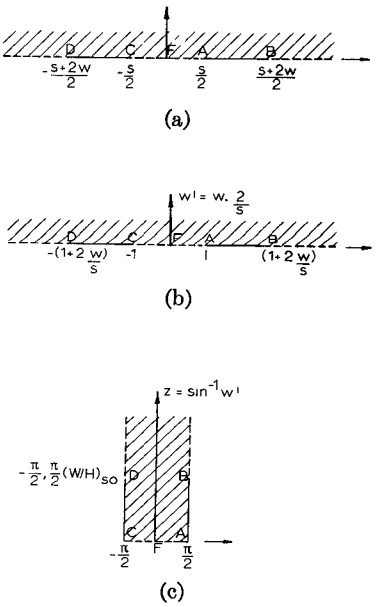

Fig. 8. Transformations for additional capacitances in odd mode. (a) w plane. (b) w' plane. (c) z plane.

i.e.,

$$(W/H)_{so} = (4/\pi)\cosh^{-1}\left(1 + 2\frac{W/H}{S/H}\right).$$

This equation is an approximation since the capacitor in Fig. 8(c) has a fringing field at BD, whereas the required capacitor does not. Also, since this capacitance is in air, it cannot be added directly onto the first term of (3). A way in which this term may be added has been found by empirical means by comparing the results with [1] and [2] and also by comparing with practical results.

In practice it is found that the influence of the second term in (3) is not highly dependent on ϵ_r and a choice of $\epsilon_r = 6$ gives accurate results over a wide range of substrate permittivities. This bonus feature is very useful because it allows the curves in Figs. 3 and 4 to be constructed independently of the substrate permittivity.

From a physical point of view in the odd-mode case, when $S/H \to \infty$ the coupled lines look like separate single lines and (3) becomes the same as (2). As $S/H \to 0$ the odd-mode impedances reduce towards zero requiring a single-line equivalent width tending to infinity.

V. COMPARISON WITH PRACTICAL AND THEORETICAL RESULTS

A number of couplers have been fabricated on 1.5-mm-thick alumina ($\epsilon_r = 9.6$). The coupled section of each coupler is one quarter-wavelength long at about 1.8 GHz. Straight 50-Ω connecting lines join the coupled section to microstrip-to-coaxial line transitions at the edge of the 50-mm × 50-mm substrate. Considerable effort has been expended on minimizing the discontinuities at the transitions and at the junction between the coupler and the 50-Ω lines. The maximum reflection coefficient for a combination of junction and transition is 0.06.

Measurements of even- and odd-mode impedances were made using the slotted-line technique described by Napoli and Hughes [8]. This slotted-line procedure consists of exciting the even and odd mode independently by means of equal-amplitude dual inputs to one end of the coupler, while terminating the other end in the output-line impedance of the coupler (50 Ω). The equal-amplitude inputs are in phase when exciting the even mode, and out of phase when exciting the odd mode. A slotted line was placed in one input line between the source and the coupler being measured. The voltage standing-wave ratio (VSWR) was found, and the input characteristic impedance calculated. The measurement was performed at the frequency at which the length of the coupled section is a quarter-wavelength at the modal phase velocity. This facilitates calculation of the modal impedance. From consideration of discontinuity effects, the measurement accuracy is estimated as ±3 percent.

The practical results are shown in Fig. 9, where a comparison is made with theoretical results obtained from the analysis procedure of Section III-B. The parameters used for the theoretical analysis were taken from measurements made on the couplers under test.

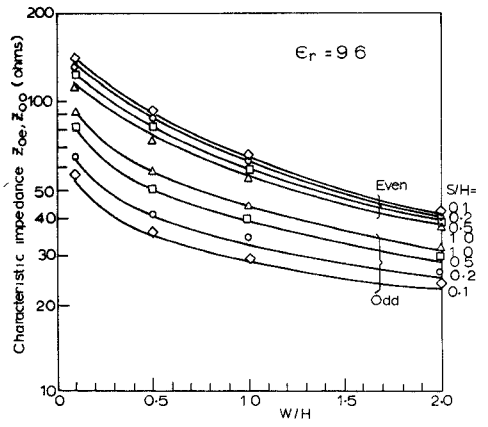

Fig. 9. Comparison of practical and theoretical results. Practical results: ◇ $S/H = 0.1$; ○ = 0.2; □ = 0.5; △ = 1.0. Theoretical results: ——.

TABLE I
COMPARISON OF THEORETICAL RESULTS $\epsilon_r = 9.6$

DIMENSIONS		BRYANT AND WEISS (REFERENCE 1)		JUDD ET AL. (REFERENCE 2)		THIS METHOD	
S/H	W/H	EVEN	ODD	EVEN	ODD	EVEN	ODD
0.1	0.1	164.1	55.4	156.7	48.0	141.7	53.8
0.1	0.5	96.2	34.5	93.3	32.3	92.1	35.2
0.1	1.0	66.5	27.8	64.8	26.6	65.0	29.0
0.1	2.0	41.7	21.6	40.8	20.7	41.3	22.7
0.2	0.1	156.0	66.1	146.5	58.2	136.0	64.6
0.2	0.5	92.2	39.9	90.0	38.5	89.0	41.1
0.2	1.0	64.5	31.6	63.0	31.5	63.4	33.1
0.2	2.0	41.0	23.7	40.1	23.0	40.7	25.1
0.5	0.1	138.4	83.5	128.1	74.5	125.2	80.9
0.5	0.5	84.5	49.7	81.9	48.0	82.2	50.8
0.5	1.0	60.5	38.1	59.0	37.1	59.7	39.5
0.5	2.0	39.4	27.4	38.5	26.9	39.2	28.7
1.0	0.1	126.0	96.6	115.6	87.1	116.4	92.5
1.0	0.5	77.4	57.7	74.8	55.8	76.1	58.3
1.0	1.0	56.5	43.2	55.0	42.3	56.2	44.3
1.0	2.0	37.6	30.1	36.7	29.7	37.6	31.2

Comparison has also been made between the theoretical results of this method and those obtained by Bryant and Weiss [1] and Judd *et al.* [2], over a wide range of ϵ_r, W/H, and S/H. Table I shows the comparison for a permittivity of $\epsilon_r = 9.6$. To facilitate this comparison the results of Bryant and Weiss for $\epsilon_r = 9.0$ were scaled to $\epsilon_r = 9.6$ by assuming that the impedance varies as $(\epsilon_r + 1)^{-1/2}$.

VI. CONCLUSIONS

By using the geometry of a single microstrip line as an intermediate step, a simple design procedure for coupled lines has been devised. The synthesis procedure given in Section III-A requires the application of just three formulas (1) which gives $(W/H)_{se}$ and $(W/H)_{so}$ in terms of the design even- and odd-mode impedances, (4) which gives S/H in terms of $(W/H)_{se}$ and $(W/H)_{so}$, and (2) which gives W/H in terms of $(W/H)_{se}$ and S/H (some optimization involving (3) may be necessary for problems involving low dielectric constants).

In the even-mode impedance case the results have been derived entirely by theoretical means. In the odd-mode case, attention has been paid to known results to provide a suitable weighting factor (independent of W/H and S/H) for a term in the equation.

The comparisons with theoretical results show that over a wide range of S/H (0.1–2.0) and W/H (0.1–2.0) the difference between this method and Judd *et al.* [2] does not exceed about 12 percent. In the odd-mode case the difference between this method and Bryant and Weiss [1] does not exceed about 6 percent, whereas for even modes their results are as much as 14 percent higher. However, a comparison between the experimental results of Napoli and Hughes [8] and Bryant and Weiss [1] also indicates that (for low values of S/H) the even-mode results of the latter are high by about 11 percent.

Coupled lines have been made and measured and the results show good agreement with this method. In obtaining the practical results, the analysis procedure (Section III-B) was used because it is easier to make the coupled lines and then measure their dimensions. However, the comparison also serves to check the synthesis procedure (Section III-A) because both the analysis and synthesis procedures are based on the same formulas.

ACKNOWLEDGMENT

The authors wish to thank the Director of Research of the Post Office for permission to make use of the information contained in this paper, and A. B. Dix of Castleton Radio Laboratories, who carried out the detailed measurements.

REFERENCES

[1] T. G. Bryant and J. A. Weiss, "Parameters of microstrip transmission lines and of coupled pairs of microstrip lines," *IEEE Trans. Microwave Theory Tech. (1968 Symposium Issue)*, vol. MTT-16, pp. 1021–1027, Dec. 1968.
[2] S. V. Judd, I. Whiteley, R. J. Clowes, and D. C. Rickard, "An analytical method for calculating microstrip transmission line parameters," *IEEE Trans. Microwave Theory Tech.*, vol. MTT-18, pp. 78–87, Feb. 1970.
[3] M. Ramadan and W. F. Westgate, "Impedance of coupled microstrip transmission lines," *Microwave J.*, vol. 14, pp. 30–35, July 1971.
[4] H. A. Wheeler, "Transmission-line properties of parallel strips separated by dielectric sheet," *IEEE Trans. Microwave Theory Tech.*, vol. MTT-13, pp. 172–185, Mar. 1965.
[5] M. V. Schneider, B. Glance, and W. F. Bodtmann, "Microwave millimeter wave hybrid integrated circuits for radio systems," *Bell Syst. Tech. J.*, vol. 48, pp. 1703–1727, July 1969.
[6] P. M. Morse and H. Fesbach, *Methods of Theoretical Physics*. New York: McGraw-Hill, 1953, sec. 4.7.
[7] L. S. Napoli and J. J. Hughes, "Foreshortening of microstrip open circuits on alumina substrates," *IEEE Trans. Microwave Theory Tech.* (Corresp.), vol. MTT-19, pp. 559–561, June 1971.
[8] ——, "Characteristics of coupled microstrip lines," *RCA Rev.*, vol. 31, pp. 479–498, Sept. 1970.

Effect of 2450-MHz Radiation on the Rabbit Eye

ARTHUR W. GUY, SENIOR MEMBER, IEEE, JAMES C. LIN, MEMBER, IEEE, PIROSKA O. KRAMAR, AND ASHLEY F. EMERY

***Abstract*—The cataractogenic effects of near-zone 2450-MHz radiation in rabbits are presented. The power deposition pattern inside the eyes and head of rabbits has been determined using a thermocouple technique. It was found that a peak absorption of 0.92 W/kg occurred between the lens of the eye and the retina for each milliwatt/square centimeter incident. Time and power-density studies indicated a cataractogenic threshold of a 150-mW/cm² incident, or 138-W/kg peak absorption behind the lens for 100 min. The threshold time decreased with increasing power density. Agreement between *in vivo* intraocular temperature measurements and finite-element computer predictions reinforces the suggestion of a thermal mechanism for microwave-induced lens opacities.**

INTRODUCTION

PRODUCTION of lens opacification in the eyes of laboratory animals by exposure to microwave radiation has been known to occur since 1948 [1]–[3]. However, the exact conditions under which these changes exhibit themselves are often subjects of discussion. While it is generally known [4]–[6] that acute exposures to high-power continuous-wave radiation cause various degrees of lens opacities at a number of frequencies, there remains the question of whether chronic exposure to low power densities or pulsed radiation of low average power is significant in the induction of cataracts. Absorption of microwave energy in the eye and consequent conversion into heat has been thought of as the principal mechanism responsible for the cataractogenic effect. However, recent reports [4],[5] suggested that some factors other than the thermal one might be responsible. These reports allude to formation of lens opacities in animals receiving repeated exposures of microwave radiation at levels believed to produce insufficient temperature rise. A large portion of past investigations were characterized by lack of quantitative rigor and produced few results useful for the purpose of scientific extrapolation to human exposures. It is essential that quantitative relationships between the physical variables of microwave radiation and the biological changes in the eye be determined in order for the animal data to be of use in predicting safe levels of human exposure.

Extending the concept of quantitative measurement of the actual fields or absorbed power in the affected tissue structure relative to the incident radiation, we have established the microwave field and power patterns both inside and outside the rabbit's head and eyes by special measurement techniques while the animals were exposed to near-zone 2450-MHz radiation from a corner reflector (dia-

Manuscript received July 1, 1974; revised January 10, 1975. This work was supported in part by the Office of Naval Research under Contract N00014-67-A-0103-0025, in part by a grant from the Association of Home Appliance Manufacturers, and in part by Social and Rehabilitation Service Grant 16-P-5681810-12.

A. W. Guy is with the Department of Rehabilitation Medicine, Bioelectromagnetics Research Laboratory, School of Medicine, University of Washington, Seattle, Wash. 98195.

J. C. Lin was with the Department of Rehabilitation Medicine, Bioelectromagnetics Research Laboratory, School of Medicine, University of Washington, Seattle, Wash. 98195. He is now with the Department of Electrical Engineering, Wayne State University, Detroit, Mich. 48202.

P. O. Kramar is with the Department of Opthalmology, School of Medicine, University of Washington, Seattle, Wash. 98195.

A. F. Emery is with the Department of Mechanical Engineering, College of Engineering, University of Washington, Seattle, Wash. 98195.